# Lipid Vesicle-Coated Complex Coacervates

Fatma Pir Cakmak, Alex T. Grigas, † and Christine D. Keating\*

Department of Chemistry, Pennsylvania State University, University Park, Pennsylvania 16802, USA. †Present Address: Department of Molecular Biophysics and Biochemistry, Yale University, New Heaven, CT 06520, United States.

#### **Abstract**

Compartmentalization by complex coacervation is important across a range of different fields including subcellular and prebiotic organization, biomedicine, food science, and personal care products. Often, lipid self-assemblies such as vesicles are also present intracellularly or in commercial formulations. A systematic understanding of how phospholipid vesicles interact with different complex coacervates could provide insight and improve control over these systems. In this manuscript, anionic phospholipid vesicles were added to a series of different complex coacervate samples in which coacervates were formed by mixing one of five polycations with one of three (poly)anions that varied in chemical structure and length. Vesicles were found to assemble at the coacervate/continuous phase interface and/or form aggregates. We report how factors such as the length and identity of the polyelectrolytes and the charge ratio of cationic to anionic moieties impacts vesicle distribution in coacervate samples. Our findings emphasize the importance of interactions between vesicles and polycations in the dilute supernatant phase for determining whether the vesicles aggregate prior to assembly at the liquid-liquid interface. Uptake of an RNA oligonucleotide (A<sub>15</sub>) was also investigated to understand the effect of these liposome coatings on diffusion into coacervate droplets. Systems in which uniform vesicle coronas

assemble around coacervate droplets without restricting entry of biomolecules such as RNAs could be of interest as bioreactors.

#### Introduction

Complex coacervation is a type of liquid-liquid phase separation (LLPS) that occurs in aqueous solutions of oppositely-charged polyelectrolytes, leading to a dense coacervate phase and a dilute supernatant phase. 1 Due to the ease of undergoing LLPS with a wide variety of different macroions, and the strong tendency of these phases to accumulate organic solutes such as biomolecules, complex coacervates are used for applications ranging from food science, <sup>2</sup> drug delivery, <sup>3-4</sup> and cosmetics <sup>5</sup> to underwater adhesives. <sup>6-7</sup> LLPS also occurs in living cells, where it is responsible for the formation of membraneless organelles including cajal bodies, P bodies and the nucleolus, and coacervation has been studied as models for both intracellular compartments and protocells. 8-11 Across these intracellular, prebiotic, and industrial uses, surfactant molecules such as lipids and their self-assemblies are often present, and in some cases amphiphile-polymer mixtures themselves undergo phase separation. 12-14 A growing body of literature suggests that interactions between intracellular liquid phases and lipid membranes are important in cell biology. For example, in T cell receptor signaling, such interactions can aid protein clustering, and in neurotransmission, positioning of synaptic vesicles at synapses can be understood in terms of their collection into a synapsin-rich phase. <sup>15-16</sup> Intracellular compartments formed by LLPS have also recently been found associated with the endoplasmic reticulum. <sup>17</sup> As the importance of LLPS in living cells becomes better understood and coacervation is increasingly incorporated into model/artificial cells and protocells, greater understanding of how lipid self-assemblies interact with complex coacervates is needed.

Liposome partitioning and interfacial assembly has been studied in aqueous twophase systems (ATPS) of neutral macromolecules such as PEG and dextran polymers, which
have two polymer-rich phases rather than a concentrated coacervate and a dilute supernatant
phase. <sup>18-19</sup> Liposome chemistry and phase composition determine how liposomes partition
between the two phases and the interface, enabling bioseparations. <sup>20-23</sup> Liposome-stabilized
Pickering emulsions of PEG/dextran two-phase systems, in which assembly of intact lipid
vesicles at the aqueous/aqueous interface prevented droplet coalescence, have been reported.
<sup>24</sup> Each liposome-coated droplet could serve as a bioreactor, with enzymatic catalysts
retained inside by equilibrium partitioning while reactants and products were able to pass
through the liposome corona. Unlike a single lipid bilayer membrane surrounding the entire
interior, the assembled vesicle coating allowed molecular transport across the interface via
spaces between the vesicles. In these studies, the liposomes used were negatively-charged
and PEGylated to prevent aggregation; at high ionic strength or in the absence of PEGylation,
liposomes were unable to stabilize the PEG/dextran ATPS Pickering emulsions. <sup>24-25</sup>

It is our interest to understand the interactions between lipid vesicles and complex coacervates, which are relevant for intracellular, biotechnological, and prebiotic compartmentalization. Lipid-based coatings on coacervate droplets have been reported for just a few coacervate compositions, including poly-L-lysine/ATP and polyU/spermine systems. <sup>11,26</sup> Mann and coworkers studied fatty acid self-assembly below the critical micelle concentration to form multilayers around coacervates as a hybrid protocell model combining these two prebiotically relevant modes of compartmentalization. The resulting fatty acid coating modified the permeability of the droplets, changing their uptake of various fluorescent molecules. <sup>11</sup> Aumiller and coworkers reported assembly of pre-existing 90-nm

diameter negatively-charged, PEGylated phospholipid vesicles around polyuridylic acid/spermine coacervates. <sup>26</sup> There, as for the liposome-stabilized ATPS emulsions described above, biomacromolecular diffusion across the liposome layer remained possible and liposomes remained intact at the interface. <sup>24-25</sup> As yet no systematic understanding of how liposomes interact with coacervates has appeared. Factors such as polycation/polyanion charge ratio, polymer length, identity and charge density of the molecules are known to play important roles in physicochemical properties of complex coacervates. <sup>27-35</sup> Here we examined how these factors might affect the interactions between complex coacervate systems and lipid vesicles.

### **Experimental Section:**

**Materials:** Poly(allylamine) hydrochloride (PAH, Mw=50kDa), poly(diallyldimethylammonium chloride) (PDADMAC, MW ~ 100 kDa), polyuridylic acid potassium salt (polyU, Mw ~600-1000 kDa), polyacryclic acid (PAA, Mw= 1.8 kDa), adenosine diphosphate sodium salt (ADP), sodium chloride, tris(hydroxymethyl)aminomethane, and HPLC grade water were all purchased from Sigma Aldrich. Poly(vinylamine) hydrochloride (PVA, Mw=25kDa) and poly(diallyldimethylammonium chloride) (PDADMAC, MW ~ 240 kDa) were purchased from Polysciences, Inc., Poly(vinylbenzyltrimethylammonium chloride) (PVTAC, MW= 100 kDa) were from Scientific Polymer Products. Calcein and Sephadex g-100 were purchased from MP Biomedicals and GE Healthcare, respectively. 1-palmitoyl-2-oleoyl-snglycero-3-phospho-L-serine (POPS), 1-palmitoyl-2-oleoyl-sn-glycero-3-phospocholine (POPC), 1-palmitoyl-2-oleoyl-sn-glycero-3-phosphoethanolamine (POPE), PE-rhodamine and 1,2-dioleoyl-sn-glycero-3-phosphoethanolamine-N-(lissamine rhodamine B sulfonyl) (ammonium salt) (Rhodamine PE) were all purchased from Avanti Polar Lipids in chloroform. In this manuscript, since the hydrophobic tails are the same for all lipids used, we refer to them by the shortened abbreviations PS, PC and PE.

Coacervate Preparation: Coacervate samples were prepared in charge concentration ratios of 10 mM (charge of the molecule×concentration of the molecule = charge concentration) with a total volume of 100 μL in HPLC grade water and 10 mM Tris pH 7.4 and 100 mM NaCl. pH of the stock solutions was fixed to 7.4 by adding NaOH or HCl. The order of addition was as follows: water, NaCl, Tris, polyanion, polycation. Samples were pipette mixed and transferred to a Corning 96 well special optics plates. Extinction spectra for were recorded for each well from 500 nm – 600 nm using a Tecan M1000 Pro microplate reader and converted to turbidity values (T, turbidity = 100 – % transmittance). <sup>36</sup> Each sample was then imaged at 100x with a Nikon Eclipse TE200 inverted optical microscope to confirm the presence of coacervate droplets. Finally, the pH for each sample was determined using the Mettler Toledo Seven Excellence pH meter by using pH Electrode InLab Ultra-Micro-ISM.

**Liposome Preparation**: Liposomes were prepared by gentle hydration followed by extrusion. Lipids were first dried into a film and hydrated in buffer overnight. For 1:1 PS: PC, 49.9 % by molarity of PS and 50 % of PC were diluted in chloroform. For 1:2:1 PS: PC: PE, 25 % by molarity of PS, 50 % by molarity of PC and 24.9 % by molarity of PE were diluted in chloroform. 0.1 % by molarity PE-rhodamine was used for fluorescence microscopy. A stream of argon gas was then used to dry the lipids into a film. 1 mL of 10

mM Tris, 100 mM NaCl buffer was added to the dried lipids and the samples were left at 40 °C overnight to hydrate. Once the lipid samples were hydrated, they were then extruded using the Avanti Polar Lipids extruder through 200 nm and then 50 nm membranes 11 times, respectively.

Zeta potential and Liposomes Size Determination: Zeta potential and size measurements were taken on the Malvern Zetasizer Nano-ZS. 1 mL samples were prepared for the zeta potential and DLS measurements. Zeta potential measurements, except for polyU systems, were taken in triplicate samples and each sample was measured three times. Due to the expense of polyU, polyU-containing samples were not prepared in triplicate, but rather measured five times with one sample. For measuring the zeta potential and size of the liposome samples,  $20~\mu L$  of the hydrated liposomes were diluted in  $980~\mu L$  of 10~mM Tris, 100~mM NaCl buffer or continuous phase of the coacervate phase.

Fluorescent Microscopy and FRAP: Coacervate samples were prepared according to the coacervation preparation section, except 10 μL of water was replaced with 10 μL of extruded liposomes, which was added last leading to 0.25 mg/mL lipid concentration. Microscope images were taken on the Leica TCS SP5 inverted confocal microscope with exciting wavelength at 543 nm. After selecting a droplet for analysis, a 10 frame pre-bleach sequence was used followed by a 5 or 10 frame bleach at 100% 458 nm, 476 nm, 488 nm, 514 nm, 543 nm and 633 nm laser power for rhodamine-labeled lipids. Regions of interest (ROI) for partial bleaching were 2 μm diameter for lipid vesicles. Whole droplet was photobleached

for RNA diffusion. For partitioning studies, calibration curves were used to determine to concentration in droplet phase.

**Fluorimeter:** Bulk fluorescence measurements were made using a Fluorolog 3-21 fluorimeter with FluorEssence software and a Wavelength Electronics temperature controller. Coacervates samples were prepared as explained and fluorescently labeled RNA (AF 647 A<sub>15</sub>) was added. Phases separated by centrifugation and fluorescence in continuous phase was measured. Calibration curves were used to determine to concentration in continuous phase. Partitioning coefficient was calculated by dividing concentration in droplet phase by continuous phase.

Calcein leakage: Liposomes were prepared by gentle hydration followed by extrusion as explained in liposome preparation section. Instead of just buffer 10 mM calcein in 10 mM Tris was added to the dried lipids and the samples were left at 40 °C overnight to hydrate. Once the lipid samples were hydrated, they were then extruded using the Avanti Polar Lipids extruder through 200 nm and then 50 nm membranes 11 times, respectively. Liposome loaded with calcein was separated by size exclusion column.<sup>37</sup> Liposome concentration in the samples was  $\sim 4.94$  nM and volume of liposomes in the sample is  $\sim 0.08 \mu L$ . <sup>38</sup>

#### Results/Discussion

Charge-charge interactions between the coacervate droplets and the lipid vesicles can be expected to be especially important in determining how these systems interact. We prepared a variety of complex coacervates spanning different polyelectrolyte chemical identities and ion-pairing strengths (Figure 1A), and also varied the polycation to polyanion

charge ratio. To test for the generality of the results, two lipid vesicle compositions were compared: 1:1 PC: PS and 1:2:1 PE: PC: PS (Figure 1B), both having hydrodynamic radii ~ 90 nm (Table S1). Zeta potentials were -34 and -27 mV for 1:1 PC: PS and 1:2:1 PE: PC: PS vesicles, respectively (Table S1). These lipid compositions were chosen in part because their adsorption on polyelectrolyte multilayer surfaces had been previously studied. <sup>26, 39</sup> In those studies, continuous supported lipid bilayers could be formed by judicious tuning of charge-charge interactions between lipid headgroups and solid-supported polyelectrolyte films. <sup>40-43</sup> We used confocal fluorescence imaging to determine the location of labeled liposomes with respect to coacervate droplets for each of the two lipid compositions added to each of the coacervate systems (each polycation/polyanion pairing at each charge ratio), 60 samples in all. In the following sections, we begin by discussing the formation of coacervates from different polyelectrolyte pairs and then discuss the impact of order-of-addition, coacervate composition, lipid headgroup composition, and cationic: anionic group charge ratio on the distribution of liposomes in these systems.

Formation of complex coacervates. We used five cationic and three anionic components to form complex coacervates for these studies (Figure 1A). All samples were prepared in 100 mM NaCl 10 mM Tris pH 7.4 buffer, at polyelectrolyte concentrations ranging from 10 mM to 30 mM in charged groups (charge concentration = charge per monomer × # monomers). Different length (poly) anions ADP, PAA (~25 mer) and polyU (~2600), in which we have a range from monomer to ~2600 bases were used while keeping polycation size relatively similar to each other. The polycations used here can be grouped into two categories based on their charge densities: PVA and PAH have high charge density (one charge per 43.07 or 57.09 g/mol, respectively), while PDADMAC and PVTAC have lower charge densities (one

charge per 126.22 or 176.28 g/mole, respectively). Two lengths of PDADMAC (n ~620 and n~1485) were compared to check for length effects. Schlenoff and coworkers have reported association constants (K<sub>a</sub>) for these polycations with the polyanion, poly(4-styrenesulfonic acid). They found that K<sub>a</sub> ranged from 17.55 and 12.92 for PVA and PAH, respectively, to 2.42 and 1.48 for PDADMAC and PVTAC, respectively. <sup>32</sup> Although we are using different anionic components here, it is reasonable to anticipate that the relative ordering of polycation affinities for a given (poly)anion may follow the same trend.

Along with the charge density, polycation: (poly)anion charge ratio was varied from 1:1 to 3:1 in an effort to facilitate assembly of negatively charged lipid vesicles around the coacervate droplets by tuning the coacervate surface charge towards more positive values. Increase of charge ratio of polycations to (poly)anions can lead to increase of polyelectrolyte concentration in the droplet phase. <sup>36</sup> Images of polyelectrolyte solutions were taken for each polycation/ (poly)anion combination at each charge ratio to determine whether coacervates were formed; representative transmission optical microscopy images for each system are shown in Figures S1-S5. In most cases coacervation was observed, with dense liquid phases visible via microscopy; visible differences between systems suggest that phase volume and wetting of the glass coverslip varied between systems. A few polycation/polyanion pairs did not form liquid phases under our experimental conditions. High charge density polycations (PVA and PAH) with polyU as the anionic component mostly formed irregularly-shaped structures that appear to be aggregates or hydrogels. An exception was 3:1 charge ratio for PAH: polyU, which formed coacervates (see Figure S1-S2). Low charge density polycations (PDADMAC and PVTAC) with ADP did not undergo phase separation under our experimental conditions at any of the charge ratios, and no structures were observed by optical microscopy (see Figure S3-S5). These findings are consistent with literature studies that generally report formation of solid aggregates or hydrogels under conditions of strongest association (e.g., higher charge density, greater multivalency, and/or lower ionic strength media), and inability to undergo coacervation for lowest association (lower charge density, lower multivalency, high ionic strength media), with coacervation observed for intermediate conditions.<sup>27, 33-34, 44</sup>

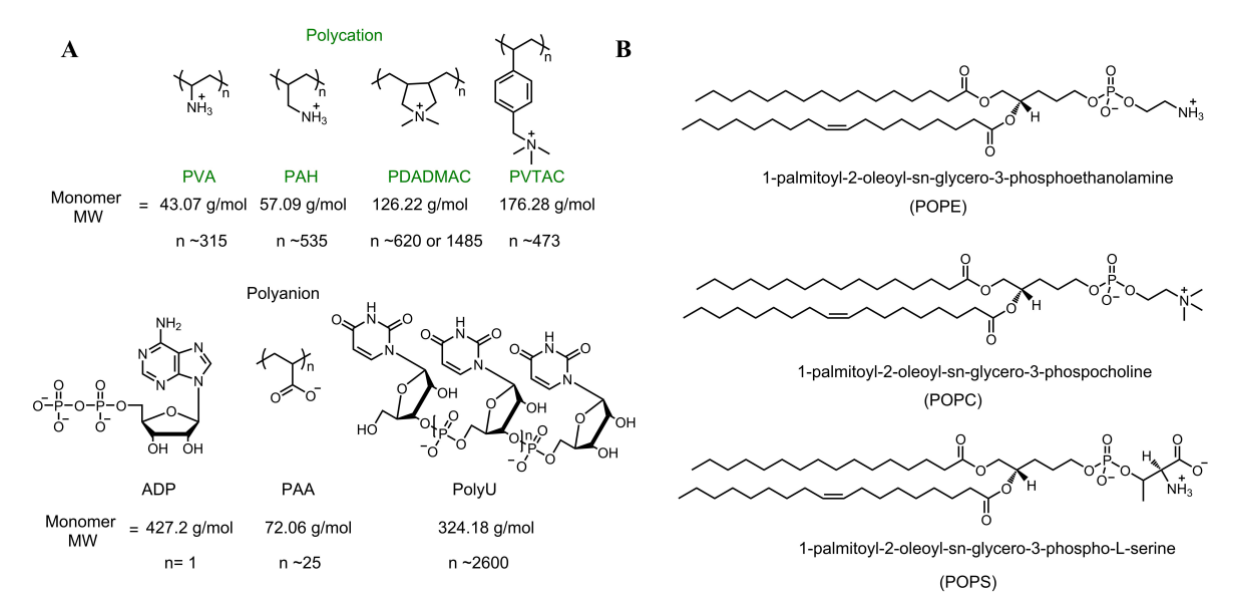
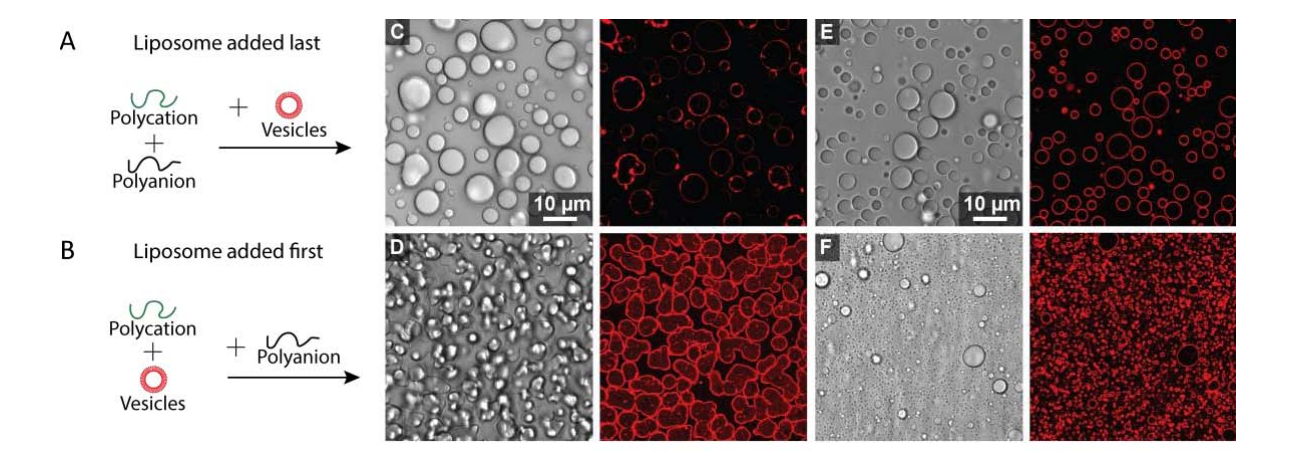


Figure 1. Structures of (A) polyelectrolytes and (B) phospholipids used. Polycations from left poly(vinylamine) (PVA), to right: poly(allyamine) (PAH), poly(diallydimethylammonium chloride) (PDADMAC, in two lengths) and poly(vinylbenzyltrimethylammonium chloride) (PVTAC). (Poly)anions from left to right: adenosine diphosphate (ADP), poly(acrylic acid) (PAA) and poly(uridylic acid) (poly U). Phospholipids POPE, POPC and POPS are further abbreviated to PE, PC and PS in the text.

We anticipated that droplet surface charge could be important in determining the interaction of coacervates with the phospholipid vesicles, which are anionic. Zeta potential measurements were taken to determine the apparent surface charge of the coacervate

droplets. At 1:1 charge ratio, PVA/ADP and PAH/ADP were positively-charged, PDADMAC 100k/PAA, PDADMAC-240k/PAA, and PVTAC/PAA were near neutral, while PAH/PAA, PVA/PAA and all of the polycation/polyU combinations had negative zeta potentials (Figure S6). These differences in zeta potential at 1:1 charge ratio reflect the differences in charge density and length for the different polyelectrolyte pairs. For instance, systems containing the smallest anion (ADP) only phase separate with high charge density polycations, and the resulting coacervates are positively charged, while the much longer polyanion, polyU produces negatively charged droplets in all of the combinations that lead to coacervation, and forms solid aggregates with the highest charge density polycations. In all cases, increasing the cation:anion charge ratio led to a more positive zeta potentials for the resulting coacervates (Figure S6).

Order of liposome to coacervate addition impacts liposome distribution. The liposomes are anionic and can be expected to interact with free polycations, potentially competing with the (poly)anions. We therefore investigated how order of addition of polyelectrolytes and lipid vesicles might change the outcome. Figure 2 compares the two scenarios tested here: adding the lipid vesicles after mixing the two polyelectrolytes to form coacervate droplets (Figure 2A) versus adding the lipid vesicles to the polycations before adding (poly)anions (Figure 2B).



**Figure 2.** Effect of order of addition: when vesicles were added last (A, C, and E) and first (B, D, and F). PVA –ADP 3:1 with 1:1 PC: PS lipid vesicles were prepared in a way when lipids (C) last and (D) first. PDADMAC 100k –PAA 1:1 with 1:2:1 PE: PC: PS lipid vesicles were prepared in a way when lipids (E) last and (F) first.

Two polymer/lipid combinations were compared for each order of addition. In all cases tested, liposomes were primarily found at the interface rather than the interior of the coacervates. Interfacial vesicle assembly around the coacervate droplets was more uniform when liposomes were added after coacervate formation than when they were present in the solution before addition of (poly)anions. For liposomes produced from 1:1 PC: PS lipids, and PVA/ADP polyelectrolyte pair at 3:1 charge ratio, coacervate droplets were more spherical and contained less internal fluorescence due to labeled lipid molecules when liposomes were added after coacervate formation (Figure 2C-D, and see Figure S7A). When liposomes were present during coacervate formation, the resulting coacervate phase was nonspherical, and contained internal labeled lipid. For the 1:2:1 PE: PC: PS lipid composition with PDADMAC-PAA polyelectrolyte pair at 1:1 charge ratio, we observed smaller droplets and slightly higher fluorescence inside of the coacervates when liposomes were added before

coacervate formation (Figure 2E-F, and see Figure S7B). Based on these observations, we maintained the "liposomes last" order of addition (Figure 2A) for all other experiments in this manuscript.

**Table 1.** Liposome distribution in coacervate samples with at 1:1 cationic: anionic group charge ratio. High (PVA and PAH) and low charge density polymers (PDADMAC and PVTAC) are listed in the order of decreasing charge density from left to right.

Liposome		Polycation					
Composition <sup>a</sup>	(Poly)anion	PVA	PAH	$PDADMAC^{b}$	PVTAC		
1:1 PC:PS	PolyU	<u></u> c	c	outside <sup>d</sup>	outside <sup>d</sup>		
	PAA	@ interface	@ interface	aggregates	aggregates		
	ADP	aggregates @ interface	@ interface	<u>e</u>	e		
1:2:1 PE:PC:PS	PolyU	c	c	outside <sup>d</sup>	outside <sup>d</sup>		
	PAA	evenly distributed	@ interface	@ interface	@ interface		
	ADP	aggregates @ interface	aggregates @ interface	<u>e</u>	e		

<sup>&</sup>lt;sup>a</sup> Lipid mole ratios used to prepare vesicles. Both recipes contained 0.1 mole% rhodamine-DOPE for visualization by fluorescence microscopy. <sup>b</sup>Table entries refer to both PDADMAC molecular weights, which showed the same trends in lipid distribution for all coacervate and lipid compositions. <sup>c</sup>Aggregates rather than coacervates formed for this polyanion/polycation pair. <sup>d</sup>Liposomes were distributed uniformly in the continuous phase but excluded from the droplet interior.

Coacervate chemistry impacts interfacial liposome assembly. Table 1 summarizes our observations for liposome distribution in coacervate samples. In general, we observed liposome assembly at the interface surrounding coacervate droplets and/or aggregation of liposomes (and, presumably, polyelectrolytes) in these systems (Table 1, Figure 3, Figure S8, Table S2 and S3). When both lipid/polymer aggregates and coacervate droplets were present, the aggregates often accumulated at interfaces around/between coacervates (Figure

<sup>&</sup>lt;sup>e</sup>No phase separation occurred for this polyanion/polycation pair.

S8C). In some cases, liposomes were somewhat uniformly distributed in the continuous phase outside of the coacervate droplets (Figure 3C). Two classes of behavior were observed, depending on which polycations were present. Coacervate systems that contained high charge density polycations (PVA and PAH) exhibited different behavior as compared to those with lower charge density polycations (PDADMAC and PVTAC) (Table 1). For example, uniform vesicle coatings formed around coacervates prepared using PAA as the polyanion when the polycation was PVA or PAH, but vesicle aggregates formed when the polycation was PDADMAC or PVTAC (for 1:1 PC: PS lipid composition). Length of the (poly)anion was also important. In general, vesicles added to coacervates containing the longest polyanion, polyU, were largely excluded from both the droplets and the interface, accumulating in the continuous phase (Table 1 and Figure 3C). We compared two different sizes of PDADMAC (molecular weights 100 kDa and 240 kDa), and saw little difference between them in terms of their coacervate-liposome interactions (Figure S9, Table S2 and S3). However, vesicle distribution when added to coacervates formed with shorter polyanions (ADP and PAA) depended on polycation type and liposome composition (Table 1 and Figure 3A-B).

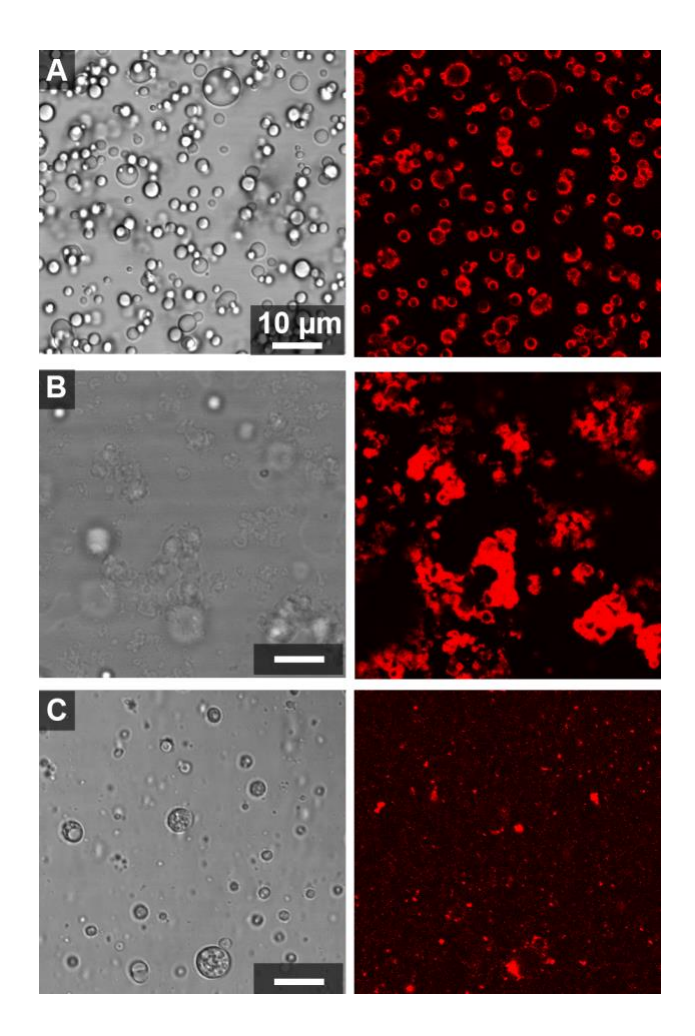


**Figure 3.** Vesicle assembly in coacervate samples formed using 1:1 PC: PS lipids at 1: 1 charge ratio of polycation to (poly)anion. Optical microscope images show transmitted light (left) and fluorescence of rhodamine-labeled lipids (right) for samples containing (A) PAH/ADP, (B) PDADMAC/PAA and (B) PDADMAC/polyU coacervates.

Effect of lipid composition: The two lipid compositions behaved similarly, but not identically, in their assembly behavior when added to coacervate samples. Differences were most apparent for coacervates that contained PAA, the polyanion of intermediate length (Table 1, Figure 4). Relatively uniform interfacial assembly of 1:1 PC: PS liposomes occurred for coacervates having high charge density polycations (PVA and PAH). In contrast, 1:2:1 PE: PC:PS liposomes formed more uniform coatings around coacervates

formed with low charge density polycations (PDADMAC and PVTAC). These differences are presumably related to the somewhat greater negative charge of the PE: PC: PS vesicles. Coacervates formed with PAA as the polyanion and either PDADMAC or PVTAC polycations have zeta potential close to 0, while coacervates formed with PVA or PAH polycations have negative zeta potentials (Figure S6). The charge density of polycations seems to play a role in handling the excess charge on coacervate droplets, resulting in the observed diversity of assembly behavior upon mixing different compositions of liposomes and coacervates. Importantly, some free polyelectrolytes and/or soluble polyelectrolyte complexes can be anticipated in the supernatant phase, which likely influence vesicle aggregation. We infer that strong electrostatic interactions between the negatively-charged vesicles and any polycations in the supernatant phase are responsible for the vesicle aggregation observed in several systems (Table 1). Although at the 1:1 charge ratio used here, both the polyanions and polycations are concentrated together into the coacervate phase, some polyelectrolyte nonetheless can be expected to remain in the supernatant at equilibrium. The relative concentrations of polycation vs. polyanion in the supernatant will depend on the strength of the ion-pairing interactions between them. 33-34

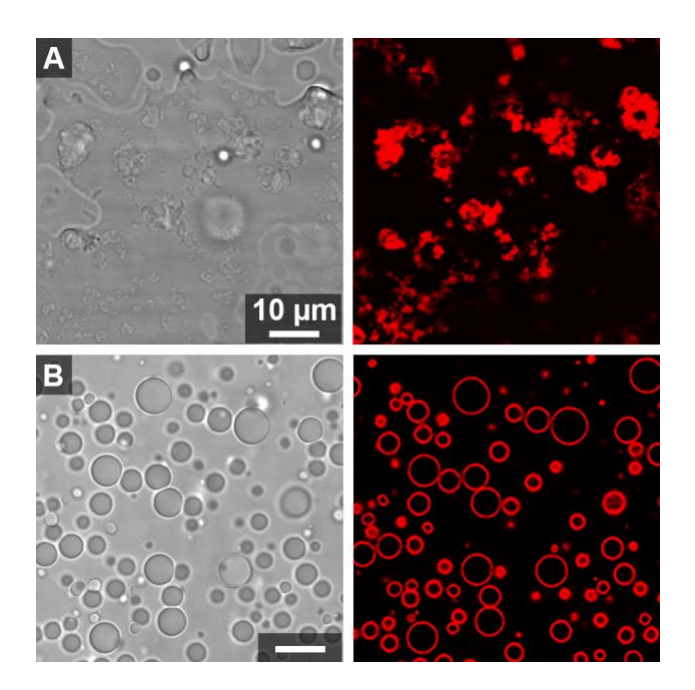


**Figure 4.** Optical microscope images showing vesicle assembly in coacervate samples formed using low charge density polycations with different compositions of lipids. Left microscope images show transmitted light and right images show fluorescence of rhodamine labeled lipids for samples containing PDADMAC/PAA, coacervate formed at 1:1 charge ratio interaction with (A) 1:1 PC: PS and (B) 1:2:1 PE: PC: PS lipid vesicles.

Excess polycations in the supernatant impact vesicle assembly on coacervates. The final variable that we evaluated was the role of charge ratio between cationic and anionic groups. For all the experiments discussed above, we maintained a 1:1 charge ratio. Here, we examine the impact of excess cationic groups at 2:1 and 3:1 charge ratios. In all cases, excess polycation resulted in positively-charged coacervate droplets, with zeta potentials much more positive for 2:1 than 1:1 ratio, but generally similar at 2:1 and 3:1 ratios (Figure S6). In principle, this additional positive charge at the surface of the coacervate droplets could be

expected to aid interfacial assembly of the negatively-charged vesicles. However, some of the excess polycation –perhaps most of it– also remains in the supernatant phase, where it can interact with vesicles prior to their interfacial assembly.

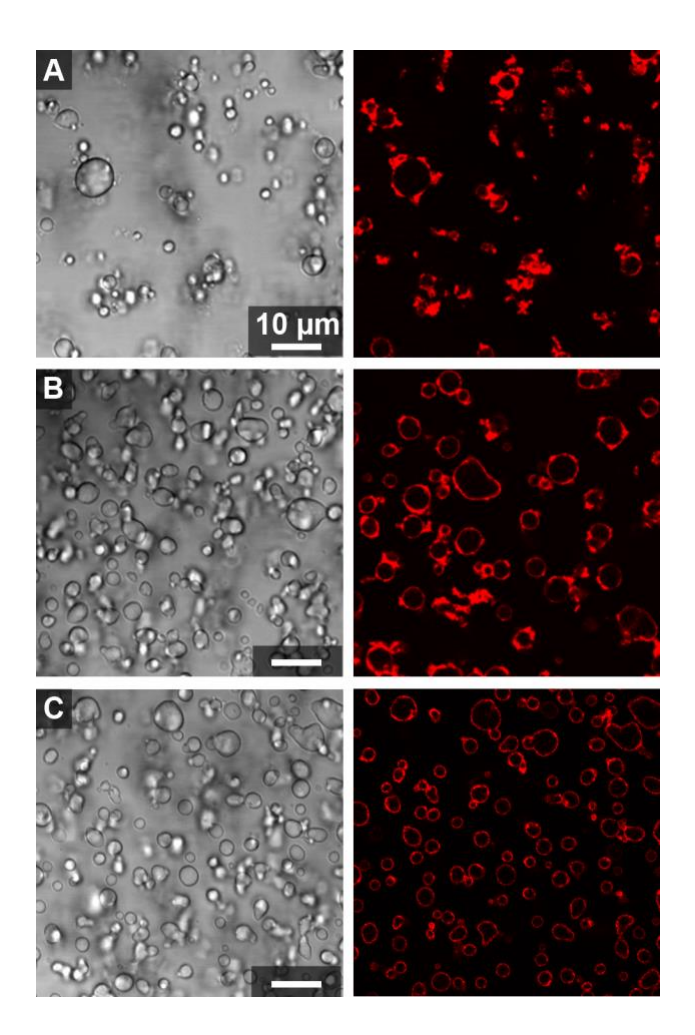


**Figure 5.** Charge ratio effect over the vesicle assembly at the interface for complex coacervates containing high charge density polycations. Left microscope images show transmitted light and right images show fluorescence of rhodamine labeled lipids for samples containing (A) PVA/ADP coacervate formed at 1:1, (B) 1:2 and (C) 1:3 charge ratio and interactions with 1:1 PC: PS lipid vesicles.

Some trends were observed in the data. For coacervate systems formed from high charge density polycations and ADP, we observed an improvement in the uniformity of interfacial vesicle coatings as we go from 1:1 to 3:1 charge ratio. Vesicle aggregates at the interface, observed for 1:1 and 2:1 charge ratios, gradually decreased, with more uniform coatings observed at 3:1 charge ratio (Figure 5 and S10). Similar results were obtained for both lipid compositions (Table S2 and S3). It is difficult to make molecular level conclusions based on imaging data alone. To better understand how the dilute continuous phase might play a role in what we observe under the microscope, we checked for evidence of polycation-induced vesicle aggregation in samples that contained only the dilute phase. This was done by centrifugation to separate the coacervate and dilute phases from each other. Dynamic light scattering (DLS) was then acquired for supernatant samples with and without added liposomes (Table 2 and Table S4). Hydrodynamic radii reported for supernatants with no added liposomes correspond to free and/or complexed polyelectrolytes. For several samples, these values are on the same order as the DLS values for the liposomes; we do not attempt to differentiate sizes of liposomes vs. polyelectrolytes and their complexes but rather have used these DLS data to check for large aggregates. We interpret hydrodynamic radii much greater than the size of either vesicles or polyelectrolytes as aggregates of the two species due to electrostatic interactions. For example, in PVA/ADP coacervate systems, micronscale aggregates are observed for charge ratios 1:1 and 2:1, but not for 3:1 (Table 2); the absence of micron-scale liposome/polyelectrolyte aggregates in the 3:1 samples is correlated with more uniform interfacial liposome assembly (Figure 5C). Smaller increases in hydrodynamic radii for liposomes in buffer vs. supernatants could be due to polyelectrolyte adsorption and/or formation of small aggregates. For the PVA/ADP system, as excess

polycation is added to shift the system from 1:1 to 3:1 charge ratio, DLS indicates a decrease from >1 micron aggregates at 1:1 and 2:1 charge ratio to ~200 nm structures at 3:1 charge ratio. At the same time, zeta potential for these structures goes from -18 to +24 and then +27 mV. These data are consistent with increasing adsorption of polycation to the vesicles approaching a saturation point after which all of the vesicles were fully-coated with polycation and therefore no longer prone to aggregating via charge-charge interactions. The 3:1 charge ratio PVA/ADP samples, which lacked >1 micron aggregates in dilute phase alone, are also the only ones that led to uniform liposome coatings around coacervate droplets in samples that contained both dilute and coacervate phases.

Table 2 summarizes data from several representative coacervate systems as a function of charge ratio; additional results for other coacervate/liposome compositions can be found in Tables S4-S9. We observed a correlation between aggregation behavior of liposomes in supernatant phase and interfacial assembly around coacervate droplets for all the systems tested: uniform vesicle coatings were possible only when largescale aggregation did not occur in the supernatant phase. There was no one "best" charge ratio in these studies. Rather, 1:1 charge ratio was best for certain systems (e.g., PDADMAC/PAA) and 3:1 was best for others (e.g., PVA/ADP). This can be rationalized as a consequence of (1) differences in supernatant polyelectrolyte content and identity for different polyelectrolyte pairs at 1:1 charge ratio, and (2) liposome-polycation interactions that lead to aggregation for incompletely-coated liposomes but provide stabilization and charge reversal for fully-coated liposomes. Across all polyelectrolyte pairs and charge ratios tested, the presence of large aggregates in supernatant studies was predictive for aggregation in coacervate samples. The

absence of large aggregates in supernatant studies usually corresponded to systems that formed uniform liposome coatings around coacervate droplets. PDADMAC/polyU at 1:1 charge ratio is an exception: no large aggregates are present in supernatant studies however the substantial negative charge on both coacervate droplets and liposomes prevented interfacial assembly.

**Table 2:** Summary of results for liposome interactions with PVA (high charge density) /mononucleotide and PDACMAC (low charge density) /PAA complex coacervates as a function of charge ratio.

Cation	Anion	Charge Ratio (+)/(-)	Zeta potential of coacervate (mV) <sup>a</sup>	Zeta potential of liposome in supernatant (mV) <sup>b</sup>	DLS of liposome in supernatant (nm) <sup>c</sup>	DLS of supernatant (nm)	Microscope Data
PVA	ADP	1:1	$+6 \pm 1.3$	-17.9 ± 1	$1871 \pm 152.8$	$126.2 \pm 31$	aggregates @ interface
	ADP	2:1	+ 14.1 ± 1.7	$+23.7 \pm 2.1$	$1788.4 \pm 67.9$	$87.9 \pm 8.6$	aggregates @ interface
	ADP	3:1	$+22.3 \pm 2.2$	+ 27± 1.7	191 ± 1.8	$107.5 \pm 2.1$	@ interface
PDACMAC	PAA	1:1	$+2.1 \pm 0.6$	-26 ± 1.1	$138.2 \pm 2.7$	$6.5 \pm 1.3$	@ interface
	PAA	2:1	+ 24.4 ± 1.3	$+6.2 \pm 0.3$	$2895.6 \pm 376.2$	$6.4 \pm 0.4$	aggregates
	PolyU	1:1	$-19.5 \pm 3.1$	-20.5 ± 0.9	$202.2 \pm 3.2$	$187.2 \pm 4.1$	evenly distributed
	PolyU	2:1	+ 9.8 ± 1.2	$-6.9 \pm 0.3$	$2529.8 \pm 105.2$	$164.5 \pm 24.5$	aggregates @ interface

<sup>a</sup> Zeta potential of turbid coacervate solutions were reported. <sup>b</sup> Data acquired for turbid complex coacervate solutions. Values should be compared with zeta potential measured in polyelectrolyte-free buffer (-33.7 and -27 for 1: 1 PC: PS and 1: 2: 1 PE: PC: PS vesicles, respectively). <sup>c</sup> Liposomes added to continuous phase rather than coacervates formed for this polyanion/polycation pair; values should be compared with liposome size in polyelectrolyte-free buffer (88.6 and 87.3 nm for 1: 1 PC: PS and 1: 2: 1 PE: PC: PS vesicles, respectively). Microscope results, zeta and DLS measurements reported were obtained with samples containing 1: 1 PC: PS lipid composition for PVA/ADP and 1: 2: 1 PE: PC: PS for PDACMAC/PAA. Error bars represent the standard deviation of three measurements made on samples.

Together, our DLS and zeta potential measurements and the microscope images point to a critical role for the dilute continuous phase, in determining how lipid vesicles will interact with different coacervate phases. When liposomes are added to the mixture, they will interact with any polyelectrolytes and/or complexes in the continuous phase prior to reaching the liquid/liquid interface around the coacervate droplets. By monitoring liposome size in continuous phase, it is possible to predict the formation of aggregates and consequently whether uniform lipid vesicle coronas can be formed around a particular coacervate composition. Perhaps an obvious solution to the problem of supernatant-induced vesicle aggregation would be to swap out the supernatant phase for a polyelectrolyte-free buffer. However, changing the supernatant phase causes re-equilibration of the samples and, at least for the systems tested here, was not a viable approach for preventing aggregation. Therefore, we suggest instead that cationic-to-anionic charge ratio can be adjusted to minimize liposome aggregation, with analysis by DLS to identify optimal charge ratios.

Adsorbed vesicles do not fuse to form supported bilayers. When lipid vesicles are exposed to silica surfaces, or surfaces covered with polyelectrolyte multilayer thin films, the vesicles

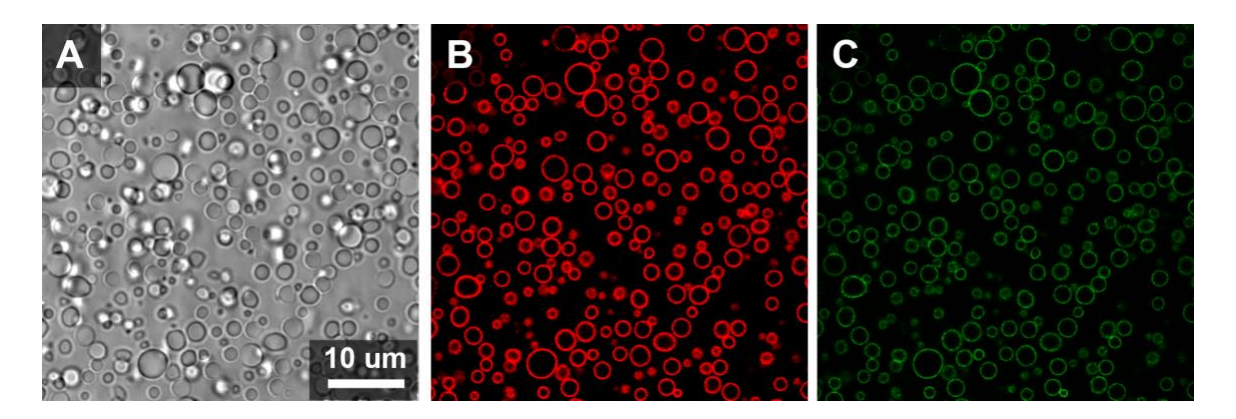


**Figure 6**. Leakage experiment for calcein loaded vesicles. Microscope images show transmitted light image (A), fluorescence channel of rhodamine labeled lipids (B) and calcein cargo for samples containing PDADMAC 100K – PAA coacervate formed at 1:1 charge ratio with 1:2:1 PE: PC: PS lipid vesicles. Fluorescence images of rhodamine labeled lipid and calcein were false colored red and green, respectively.

can fuse to form supported lipid bilayers. <sup>45-46</sup> Therefore it is of interest to determine whether such a bilayer could be forming around our coacervate droplets. In a previous study where lipid vesicles were adsorbed to RNA/spermine coacervate droplets, it was possible to verify that vesicles remained intact (rather than fusing to form a bilayer) by thermally dissolving the coacervates to release the vesicles. <sup>26</sup> The coacervates used in the present study were not sufficiently thermally sensitive to allow such experiments. A second test for the structure of the lipid vesicles at the interface is to measure lipid diffusion. More rapid lipid diffusion in the plane of the membrane can be used to show formation of a lipid bilayer from adsorbed vesicles at a solid interface. <sup>47-49</sup> We therefore tested each of the coacervate/vesicle systems that formed some kind of coating around the coacervate droplet with or without any aggregation by fluorescence recovery after photobleaching (FRAP). We found no fluorescence recovery for any of the systems tested even after ~ 12 minutes (Figure S11).

This indicates not only that lipid bilayers had not formed around the coacervate droplets, but also a lack of vesicle diffusion at the interface, similar to what has been seen previously for several aqueous/aqueous interfaces.<sup>24, 26</sup> We further loaded liposomes with calcein dye to check for leakage, which would indicate vesicle disruption. We used PDADMAC 100k/PAA coacervates formed at 1:1 charge ratio with 1:2:1 PE: PC: PS lipid vesicles as a model system. Calcein fluorescence was found to arise from the coacervate/continuous phase interface, colocalized with emission from rhodamine-labeled lipid headgroups (Figure 6). We did not observe calcein in either the continuous or coacervate phases. As a control experiment, we also imaged a sample to which we added free calcein dye without liposomes to the coacervates to assess whether a large fraction of the total encapsulated calcein may have been released, and to ensure that unencapsulated calcein did not interfacially associate. Signal from calcein dye as found uniformly partitioned in the continuous phase (Figure S12). Based on these two experiments, we conclude that interfacially-adsorbed vesicles at the PDADMAC/PAA coacervate/continuous phase interface remain intact. The lack of any evidence for fusion of interfacial lipid vesicles to form a continuous lipid bilayer is perhaps a bit surprising since supported lipid bilayers have been formed successfully on solidsupported polyelectrolyte multilayer films. Complex coacervates, while often generated with the same molecules and driven by the same ion pairing interactions that are used in layer-bylayer growth of polyelectrolyte multilayers, have several potentially important distinctions. The presence of soluble polyelectrolytes and complexes in the dilute phase is perhaps the most significant of these, as vesicles coated with polyelectrolytes may be unable to fuse into a continuous bilayer. Additionally, the sharpness and organization at the interface can be expected to be less well defined for coacervate droplets as compared to solid-supported multilayer films. We hypothesized based on literature that the lipid vesicles are intact at the coacervate/dilute phase interface (Figure 7) and as such that diffusion across this interface might be unimpeded by their presence.<sup>24-26</sup>

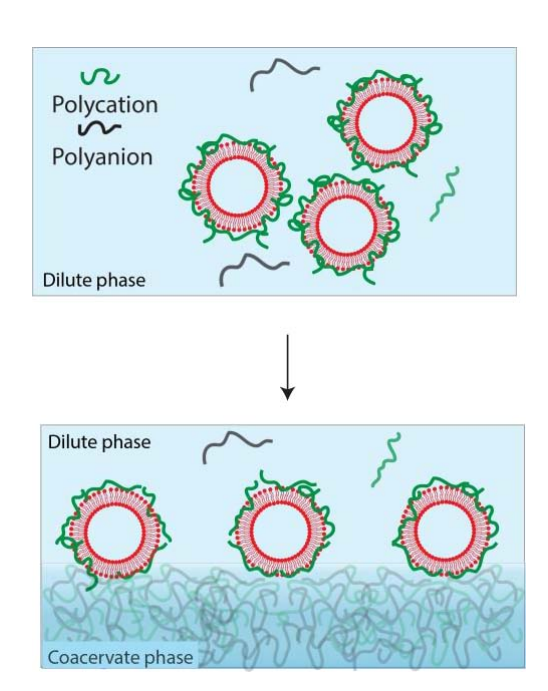


**Figure 7.** Suggested interfacial structure for liposome-coated coacervates.

RNA uptake and partitioning in vesicle-coated coacervates. We investigated the permeability of the vesicle coronas around the coacervate droplets by using fluorescently labeled A<sub>15</sub> RNA (15 repeats of adenosine). One representative system has been chosen from each of high charge density and low charge density polycations systems. PVA-ADP at 3: 1 charge ratio coated with 1:1 PC: PS and PDADMAC-PAA at 1:1 charge ratio coated with 1:2:1 PE: PC: PS were the systems used for diffusion studies. In order to eliminate the mechanical force applied at the time of mixing, coacervate samples with lipid vesicle coating were prepared and put first on the glass slide, addition of fluorescently labeled A<sub>15</sub> RNA on the sample followed. After ~ 4 min., fluorescently labeled RNA concentrated in the liposome

coated coacervate droplets (PDADMAC 100 k-PAA) and reached its maximum fluorescence value as a result of equilibrium partitioning (Figure 8 and S13). Partitioning of the fluorescently labeled RNA into liposome coated coacervate droplet has been observed for both of the systems that have been tested (Figure S14). Partition coefficients were calculated for both the PVA-ADP and PDADMAC-PAA systems with and without liposome coronas by dividing the concentration of labeled A<sub>15</sub> RNA in droplets, determined from confocal microscopy, by its concentration in the continuous phase, determined by bulk fluorescence (Table S10). The coacervate phase volumes, which are difficult to know with precision, are not needed to determine K in this way. Table 3 summarizes the results. When no liposomes are present, the labeled RNA accumulates in both cases, but more strongly in the PVA-ADP than PDADMAC-PAA coacervates (K ~3900 and ~600, respectively). Stronger partitioning into the PVA-ATP coacervates is consistent with both the stronger ion pairing interactions between the PVA and the RNA, and the lower multivalency of the anions that must be displaced to facilitate these polycation-RNA interactions (ADP vs PAA). Additionally, the PVA-ADP system used here has excess polycation (3:1 charge ratio), while the PDADMAC-PAA is charge-balanced. When liposomes were present, K was substantially reduced, by ~26% for the PVA-ADP system and ~44% for the PDADMAC-PAA system. This can be understood in terms of the anionic surface charge of the vesicles, which now competes with the labeled RNA for binding with coacervate polycations.

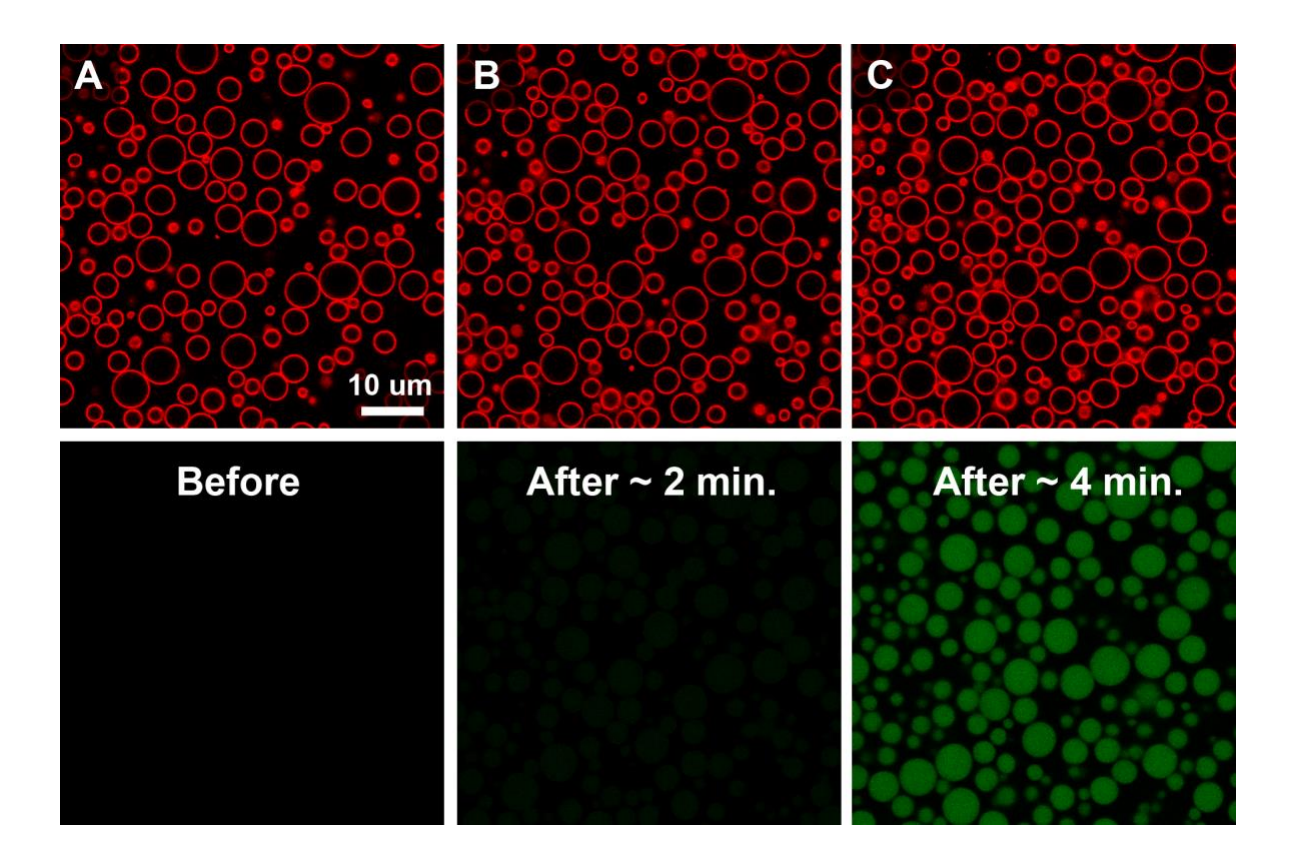


**Figure 8**. RNA diffusion through vesicle assembly at the interface. Upper panel of microscope images show fluorescence channel of rhodamine labeled lipids and bottom panel shows fluorescently labeled RNA for samples containing PDADMAC 100K – PAA coacervate formed at 1:1 charge ratio with 1:2:1 PE: PC: PS lipid vesicles (A) before and (B) after 2 minutes and (C) 4 minutes adding AF-647 A<sub>15</sub>. Fluorescence images of rhodamine labeled lipid and AF-647 RNA were false colored red and green, respectively.

Finally, fluorescence recovery experiments were performed to better understand how the liposome coatings affect the ability of RNA oligonucleotides to enter the coacervates. Labeled A<sub>15</sub> RNA was used as the probe molecule, and FRAP experiments were performed for coacervate droplets with and without a liposome corona, comparing the same two coacervate systems as used above in partitioning experiments. Entire droplets were bleached in order to follow recovery via diffusion across the coacervate/continuous phase interface.

Mobile fraction refers to the fluorescently labeled RNA that diffuses into the bleached region. In the absence of the liposome coating, the PVA-ADP system has slower and less complete recovery than the PDADMAC-PAA system, which is consistent with the higher partitioning coefficient in the PVA-ADP system. Labeled RNAs with stronger ion-pairing interactions to the polycations can be expected to exchange more slowly with their unbleached counterparts in the dilute phase. Stronger partitioning also means that less unbleached RNAs are available in the dilute phase. When liposome coronas are present around the coacervate droplets, recovery for the PVA-ADP system is greatly reduced, with mobile fraction dropping from 54% to only 16% (Table 3). In contrast, the PDADMAC-PAA system shows little change, and even a slight increase in recovery (Figure 9). The dramatic change in the mobile phase for PVA-ADP system may be related to interaction between the labeled RNA and the liposome coating; in separate experiments, we have observed colocalization of the labeled RNA with the liposomes at early times after mixing (Figure S15 and S16). Nonetheless, the remaining mobile fraction of labeled RNA had faster (3x) recovery for liposome-coated versus uncoated droplets. In contrast, the apparent diffusion coefficient was decreased (1/2x)for liposome coated PDADMAC-PAA coacervates. The observed differences in how the liposome corona impacted RNA transport into the vesicles could be due to differences in the lipid compositions (1:2:1 PE: PC: PS and 1:1 PC: PS) impacting liposome-RNA interactions, and/or could result from differences in RNA interactions with the coacervate compositions. Additional studies would be needed to fully characterize how the liposome layers and coacervate compositions together determine FRAP recovery in these systems. The results shown here indicate that liposome coronas that appear superficially similar by optical microscopy may have quite different functional performance.

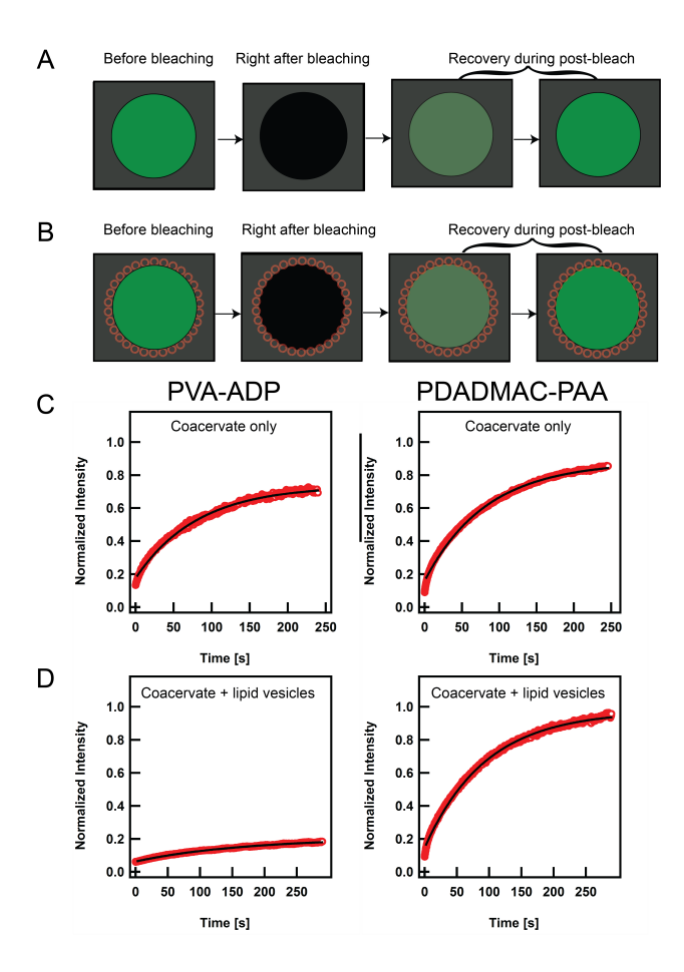


**Figure 9.** Fluorescence recovery after photobleach scheme and results. Selected droplets were fully photobleached and fluorescence recovery monitored over time for the droplets of interest (A, B). Fluorescence recovery for PVA/ADP @ 3:1 charge ratio and PDADMAC 100k/PAA @ 1:1 charge ratio coacervate droplets from left to right in panel (C), same composition of coacervates when they mixed with vesicles (1:1 PC: PS and 1:2:1 PE: PC: PS, respectively) (D). Droplet diameters were ranged from 4 to 9 μm.

**Table 3.** FRAP results and partitioning coefficients.

Coacervate system	Mobile Fraction	Half-life, τ <sub>1/2</sub> (s)	Apparent Diffusion Coefficient (μm <sup>2</sup> s <sup>-1</sup> )	Partitioning coefficients <sup>a</sup>
PVA- ADP	$0.54 \pm 0.17$	$79.2 \pm 30.3$	$0.011 \pm 0.003$	$3898 \pm 750$
Liposome coated	$0.16 \pm 0.03$	$114.7 \pm 13.3$	$0.031 \pm 0.006$	$2869 \pm 25$
PDADMAC- PAA	$0.70 \pm 0.04$	$66.3 \pm 7.6$	$0.047 \pm 0.004$	$597 \pm 58$
Liposome coated	$0.79 \pm 0.02$	$63.5 \pm 10.7$	$0.019 \pm 0.003$	$333~\pm~6$

<sup>&</sup>lt;sup>a</sup>Concentrations for labeled A<sub>15</sub> RNA in the coacervate and dilute phases can be found in Table S10.

#### **Conclusions**

The findings reported here provide insight into how complex coacervate composition impacts the formation of uniform liposome coatings, liposome aggregates, or combinations thereof. Such insight is important across diverse fields where both coacervates and lipid assemblies are present, from commercially-important emulsions to drug delivery and intracellular condensates. Lipid vesicles readily accumulate at the interface between complex coacervate droplets and dilute supernatant phase, particularly when added after coacervate formation rather than being allowed to compete for polycation interactions with polyanions prior to coacervate formation. Whether the interfacial layer appears uniform at the scale of fluorescence microscopy depends on whether vesicles are stable to aggregation in the dilute continuous phase. In many cases, excess polycation in the dilute phase results in vesicle aggregation prior to assembly at the interface. We found that it was often possible to identify conditions for vesicle stability by varying the ratio of charged groups, although the optimal

charge ratio was dependent upon which polycation/polyanion pair was used. The results generally fell into two classes: the two high charge density polycations (PVA 25k and PAH 50k) gave very similar results to each other in each set of experiments, as did the three low charge density polycations (PDADMAC 100k, PDADMAC 240k, and PVTAC 100k). We saw the most uniform interfacial vesicle assembly for the 1:1 PC:PS lipid composition when using high charge density polycations, while the 1:2:1 PE:PC:PS lipid composition resulted in uniform assembly for any of the low charge density polycations, but only when paired with PAA as the polyanion, and only at 1:1 charge ratio. None of the coacervate systems in which polyU served as the polyanion led to uniform vesicle assembly with either liposome composition. The polyU was the highest MW polyanion used here, which appeared to be related to electrostatic repulsion of vesicles from negatively-charged coacervate droplets at the only charge ratios where they were not aggregated. Testing for, and minimizing, vesicle aggregation in the dilute continuous phase can be recommended as a viable route to forming uniform vesicle assemblies around coacervate droplets. We note that steric repulsion, for example in the form of PEGylated lipid headgroups, was not used for any of the experiments reported here, but would likely aid in production of uniform layers and is not expected to prevent interfacial vesicle assembly.<sup>26</sup> Examples of uniform interfacial assemblies representing one high and one low charge density polycation coacervate systems were further evaluated to determine whether the vesicles served as a barrier to entry/egress of a fluorescently-labeled RNA oligomer. We observed system-specific differences in the mobile fraction, however in both cases, externally added RNA could pass the interface and accumulate inside the coacervate droplets. Further analysis of the most promising system in

terms of interfacial uniformity and RNA oligo mobility (1:1 PDADMAC/PAA) indicated that interfacially adsorbed vesicles remain intact, without loss of their internal contents.

Our results highlight the importance of the dilute supernatant phase in determining how lipid vesicles distribute and assemble in complex coacervate samples. The possibility of active participation of the dilute phase is often overlooked in coacervate studies but in the work presented here it was the determining factor in whether uniform vesicle coronas could assemble around coacervate droplets. Presumably the presence of free polyelectrolytes and soluble polyelectrolyte complexes in the dilute phase will impact other aspects of complex coacervate behavior as well. For example, partitioning of charged solutes may be impacted by ion-pairing interactions in the supernatant prior to reaching the coacervate droplets. Dilute phase polyelectrolyte content can be expected to increase with unequal cationic-anionic charge ratios, unmatched polymer lengths or charge densities, lower polyelectrolyte ion-pairing strengths, higher solution ionic strength, and other factors.<sup>29,50</sup>

#### ASSOCIATED CONTENT

**Supporting Information**. The Supporting Information is available free of charge on the ACS Publications website at DOI:

(PDF) includes: Microscope images of coacervate formation, zeta potential graphs of coacervates, size and zeta potential of different liposome compositions, fluorescence and DIC images of coacervate and liposome mixtures, line intensity graphs and summary tables of microscopy observations and zeta potential of the systems and partitioning.

AUTHOR INFORMATION

Corresponding Author

\* Email: keating@chem.psu.edu

Present Addresses:

† A.T.G.: Department of Molecular Biophysics and Biochemistry, Yale University, New

Heaven, CT 06520, United States.

**Author Contributions:** 

FPC and ATG performed the experiments. FPC and CDK conceived and designed the

experiments and analyzed the data. FPC and CDK wrote the paper, with contributions from

ATG.

**Funding Sources** 

This work was primarily supported by the NASA Exobiology program, grant

80NSSC17K0034, with additional support from the National Science Foundation grant

CHE-1844313 - RoL: RAISE: DESYN-C3. Undergraduate researcher ATG was supported

by an award from the Penn State University Eberly College of Science and by a Rodney A.

Erickson Discovery Grant.

Notes

The authors declare no competing financial interests.

References

1. de Jong, H. G. B.; Kruyt, H. R., Coacervation (Partial miscibility on colloid systems)

(Preliminary communication). P K Akad Wet-Amsterd 1929, 32 (6/10), 849-856.

33

- 2. Schmitt, C.; Sanchez, C.; Desobry-Banon, S.; Hardy, J., Structure and technofunctional properties of protein-polysaccharide complexes: A review. *Crit Rev Food Sci* **1998**, *38* (8), 689-753.
- 3. Kataoka, K.; Harada, A.; Nagasaki, Y., Block copolymer micelles for drug delivery: design, characterization and biological significance. *Adv Drug Deliv Rev* **2001,** *47* (1), 113-31.
- 4. Kakizawa, Y.; Kataoka, K., Block copolymer micelles for delivery of gene and related compounds. *Adv Drug Deliv Rev* **2002**, *54* (2), 203-22.
- 5. Gouin, S., Microencapsulation: industrial appraisal of existing technologies and trends. *Trends Food Sci Tech* **2004**, *15* (7-8), 330-347.
- 6. Shao, H.; Bachus, K. N.; Stewart, R. J., A Water-Borne Adhesive Modeled after the Sandcastle Glue of P-californica. *Macromol Biosci* **2009**, *9* (5), 464-471.
- 7. Hwang, D. S.; Zeng, H. B.; Srivastava, A.; Krogstad, D. V.; Tirrell, M.; Israelachvili, J. N.; Waite, J. H., Viscosity and interfacial properties in a mussel-inspired adhesive coacervate. *Soft Matter* **2010**, *6* (14), 3232-3236.
- 8. Li, P. L.; Banjade, S.; Cheng, H. C.; Kim, S.; Chen, B.; Guo, L.; Llaguno, M.; Hollingsworth, J. V.; King, D. S.; Banani, S. F.; Russo, P. S.; Jiang, Q. X.; Nixon, B. T.; Rosen, M. K., Phase transitions in the assembly of multivalent signalling proteins. *Nature* **2012**, *483* (7389), 336-U129.
- 9. Protter, D. S. W.; Parker, R., Principles and Properties of Stress Granules. *Trends Cell Biol* **2016**, *26* (9), 668-679.
- 10. Shin, Y.; Brangwynne, C. P., Liquid phase condensation in cell physiology and disease. *Science* **2017**, *357* (6357).

- 11. Dora Tang, T. Y.; Rohaida Che Hak, C.; Thompson, A. J.; Kuimova, M. K.; Williams, D. S.; Perriman, A. W.; Mann, S., Fatty acid membrane assembly on coacervate microdroplets as a step towards a hybrid protocell model. *Nat Chem* **2014**, *6* (6), 527-33.
- 12. Hansson, P.; Lindman, B., Surfactant-polymer interactions. *Curr Opin Colloid In* **1996,** *I* (5), 604-613.
- 13. Guillemet, F.; Piculell, L., Interactions in Aqueous Mixtures of Hydrophobically-Modified Polyelectrolyte and Oppositely Charged Surfactant Mixed Micelle Formation and Associative Phase-Separation. *J Phys Chem-Us* **1995**, *99* (22), 9201-9209.
- 14. Piculell, L.; Lindman, B., Association and Segregation in Aqueous Polymer/Polymer, Polymer Surfactant, and Surfactant Surfactant Mixtures Similarities and Differences. *Adv Colloid Interfac* **1992**, *41*, 149-178.
- 15. Milovanovic, D.; Wu, Y. M.; Bian, X.; De Camilli, P., A liquid phase of synapsin and lipid vesicles. *Science* **2018**, *361* (6402), 604-+.
- 16. Su, X. L.; Ditlev, J. A.; Hui, E. F.; Xing, W. M.; Banjade, S.; Okrut, J.; King, D. S.; Taunton, J.; Rosen, M. K.; Vale, R. D., Phase separation of signaling molecules promotes T cell receptor signal transduction. *Science* **2016**, *352* (6285), 595-599.
- 17. Ma, W. R.; Mayr, C., A Membraneless Organelle Associated with the Endoplasmic Reticulum Enables 3 'UTR-Mediated Protein-Protein Interactions. *Cell* **2018**, *175* (6), 1492-+.
- 18. Aumiller, W. M.; Keating, C. D., Experimental models for dynamic compartmentalization of biomolecules in liquid organelles: Reversible formation and partitioning in aqueous biphasic systems. *Adv Colloid Interfac* **2017**, *239*, 75-87.

- 19. Poudyal, R. R.; Cakmak, F. P.; Keating, C. D.; Bevilacqua, P. C., Physical Principles and Extant Biology Reveal Roles for RNA Containing Membraneless Compartments in Origins of Life Chemistry. *Biochemistry-Us* **2018**, *57* (17), 2509-2519.
- 20. Fernandes, S.; Johansson, G.; Hatti-Kaul, R., Purification of recombinant cutinase by extraction in an aqueous two-phase system facilitated by a fatty acid substrate. *Biotechnol Bioeng* **2001**, *73* (6), 465-475.
- 21. Hatti-Kaul, R., Aqueous two-phase systems A general overview. *Mol Biotechnol* **2001,** *19* (3), 269-277.
- 22. Belfrage, P.; Vaughan, M., Simple Liquid-Liquid Partition System for Isolation of Labeled Oleic Acid from Mixtures with Glycerides. *J Lipid Res* **1969**, *10* (3), 341-&.
- 23. Ishii, F.; Takamura, A.; Ishigami, Y., Procedure for Preparation of Lipid Vesicles (Liposomes) Using the Coacervation (Phase-Separation) Technique. *Langmuir* **1995**, *11* (2), 483-486.
- 24. Dewey, D. C.; Strulson, C. A.; Cacace, D. N.; Bevilacqua, P. C.; Keating, C. D., Bioreactor droplets from liposome-stabilized all-aqueous emulsions. *Nat Commun* **2014**, *5*, 4670.
- 25. Cacace, D. N.; Rowland, A. T.; Stapleton, J. J.; Dewey, D. C.; Keating, C. D., Aqueous Emulsion Droplets Stabilized by Lipid Vesicles as Microcompartments for Biomimetic Mineralization. *Langmuir* **2015**, *31* (41), 11329-38.
- 26. Aumiller, W. M., Jr.; Pir Cakmak, F.; Davis, B. W.; Keating, C. D., RNA-Based Coacervates as a Model for Membraneless Organelles: Formation, Properties, and Interfacial Liposome Assembly. *Langmuir* **2016**, *32* (39), 10042-10053.

- 27. Chollakup, R.; Smitthipong, W.; Eisenbach, C. D.; Tirrell, M., Phase Behavior and Coacervation of Aqueous Poly(acrylic acid)—Poly(allylamine) Solutions. *Macromolecules* **2010**, *43* (5), 2518-2528.
- 28. Krogstad, D. V.; Lynd, N. A.; Choi, S.-H.; Spruell, J. M.; Hawker, C. J.; Kramer, E. J.; Tirrell, M. V., Effects of Polymer and Salt Concentration on the Structure and Properties of Triblock Copolymer Coacervate Hydrogels. *Macromolecules* **2013**, *46* (4), 1512-1518.
- 29. Li, L.; Srivastava, S.; Andreev, M.; Marciel, A. B.; de Pablo, J. J.; Tirrell, M. V., Phase Behavior and Salt Partitioning in Polyelectrolyte Complex Coacervates. *Macromolecules* **2018**, *51* (8), 2988-2995.
- 30. Priftis, D.; Tirrell, M., Phase behaviour and complex coacervation of aqueous polypeptide solutions. *Soft Matter* **2012**, *8* (36), 9396-9405.
- 31. Priftis, D.; Xia, X.; Margossian, K. O.; Perry, S. L.; Leon, L.; Qin, J.; de Pablo, J. J.; Tirrell, M., Ternary, Tunable Polyelectrolyte Complex Fluids Driven by Complex Coacervation. *Macromolecules* **2014**, *47* (9), 3076-3085.
- 32. Fu, J.; Fares, H. M.; Schlenoff, J. B., Ion-Pairing Strength in Polyelectrolyte Complexes. *Macromolecules* **2017**, *50* (3), 1066-1074.
- 33. Spruijt, E.; Westphal, A. H.; Borst, J. W.; Cohen Stuart, M. A.; van der Gucht, J., Binodal Compositions of Polyelectrolyte Complexes. *Macromolecules* **2010**, *43* (15), 6476-6484.
- 34. van der Gucht, J.; Spruijt, E.; Lemmers, M.; Cohen Stuart, M. A., Polyelectrolyte complexes: bulk phases and colloidal systems. *J Colloid Interface Sci* **2011**, *361* (2), 407-22.

- 35. Radhakrishna, M.; Basu, K.; Liu, Y. L.; Shamsi, R.; Perry, S. L.; Sing, C. E., Molecular Connectivity and Correlation Effects on Polymer Coacervation. *Macromolecules* **2017**, *50* (7), 3030-3037.
- 36. Frankel, E. A.; Bevilacqua, P. C.; Keating, C. D., Polyamine/Nucleotide Coacervates Provide Strong Compartmentalization of Mg2+, Nucleotides, and RNA. *Langmuir* **2016**, *32* (8), 2041-2049.
- 37. Jin, L.; Engelhart, A. E.; Adamala, K. P.; Szostak, J. W., Preparation, Purification, and Use of Fatty Acid-containing Liposomes. *Jove-J Vis Exp* **2018**, (132).
- 38. Nilsson, T.; Lundin, C. R.; Nordlund, G.; Adelroth, P.; von Ballmoos, C.; Brzezinski, P., Lipid-mediated Protein-protein Interactions Modulate Respiration-driven ATP Synthesis. *Sci Rep-Uk* **2016**, *6*.
- 39. Fischlechner, M.; Zaulig, M.; Meyer, S.; Estrela-Lopis, I.; Cuéllar, L.; Irigoyen, J.; Pescador, P.; Brumen, M.; Messner, P.; Moya, S.; Donath, E., Lipid layers on polyelectrolyte multilayer supports. *Soft Matter* **2008**, *4* (11), 2245.
- 40. Reviakine, I.; Brisson, A., Formation of supported phospholipid bilayers from unilamellar vesicles investigated by atomic force microscopy. *Langmuir* **2000**, *16* (4), 1806-1815.
- 41. Cha, T.; Guo, A.; Zhu, X. Y., Formation of supported phospholipid bilayers on molecular surfaces: Role of surface charge density and electrostatic interaction. *Biophys J* **2006,** *90* (4), 1270-1274.
- 42. Dimitrievski, K.; Kasemo, B., Influence of Lipid Vesicle Composition and Surface Charge Density on Vesicle Adsorption Events: A Kinetic Phase Diagram. *Langmuir* **2009**, 25 (16), 8865-8869.

- 43. Kohler, G.; Moya, S. E.; Leporatti, S.; Bitterlich, C.; Donath, E., Stability and fusion of lipid layers on polyelectrolyte multilayer supports studied by colloidal force spectroscopy. *Eur Biophys J Biophy* **2007**, *36* (4-5), 337-347.
- 44. Overbeek, J. T.; Voorn, M. J., Phase separation in polyelectrolyte solutions; theory of complex coacervation. *J Cell Physiol Suppl* **1957**, *49* (Suppl 1), 7-22; discussion, 22-6.
- 45. Begley, T. P.; Kiessling, V.; Domanska, M. K.; Murray, D.; Wan, C.; Tamm, L. K., Supported Lipid Bilayers. In *Wiley Encyclopedia of Chemical Biology*, 2008.
- 46. Richter, R. P.; Berat, R.; Brisson, A. R., Formation of solid-supported lipid bilayers: An integrated view. *Langmuir* **2006**, *22* (8), 3497-3505.
- 47. Fischlechner, M.; Zaulig, M.; Meyer, S.; Estrela-Lopis, I.; Cuellar, L.; Irigoyen, J.; Pescador, P.; Brumen, M.; Messner, P.; Moya, S.; Donath, E., Lipid layers on polyelectrolyte multilayer supports. *Soft Matter* **2008**, *4* (11), 2245-2258.
- 48. Wagner, M. L.; Tamm, L. K., Tethered polymer-supported planar lipid bilayers for reconstitution of integral membrane proteins: Silane-polyethyleneglycol-lipid as a cushion and covalent linker. *Biophys J* **2000**, *79* (3), 1400-1414.
- 49. Almeida, P. F. F.; Vaz, W. L. C.; Thompson, T. E., Lateral Diffusion in the Liquid-Phases of Dimyristoylphosphatidylcholine Cholesterol Lipid Bilayers a Free-Volume Analysis. *Biochemistry-Us* **1992**, *31* (29), 6739-6747.
- 50. Chodankar, S.; Aswal, V. K.; Kohlbrecher, J.; Vavrin, R.; Wagh, A. G., Structural study of coacervation in protein-polyelectrolyte complexes. *Phys Rev E* **2008**, *78* (3).

## **TOC Graphic:**

